Evidence for P_b center-hydrogen complexes after subjecting PMOS devices to NBTI stress – a combined DCIV/SDR study

Thomas Aichinger
Pennsylvania State University
Semiconductor Spectroscopy Lab
State College, PA
phone: 01-814-404-0039; email: txa23@psu.edu

Patrick M. Lenahan
Pennsylvania State University
Semiconductor Spectroscopy Lab
State College, PA

Tibor Grasser
Technical University of Vienna
Institute for Microelectronics
Wien, Austria

Gregor Pobegen
Kompetenzzentrum Automobil- und Industrieelektronik (KAI)
Villach, Austria

Michael Nelhiebel
Infineon Technologies Austria
Villach, Austria

Abstract— **We study deep level defects at the Si/SiO_2 interface of 30nm and 5nm SiO_2 PMOS devices after negative bias temperature stress (NBTS). Electrical characterization using the direct-current current-voltage (DCIV) technique reveals two defects with different energy levels, recovery and degradation dynamics. To investigate their micro-physical nature, we perform spin dependent recombination (SDR). Besides conventional P_b centers we also find evidence for P_b center-hydrogen complexes.**

Spin dependent recombination, NBTI, P_b center, hydrogen

INTRODUCTION

Since the discovery of the negative bias temperature instability (NBTI) in silicon metal oxide semiconductor field effect transistors (MOSFETs) in 1977 [1] many different aspects of the degradation mechanism were revealed and discussed in numerous publications [2-4]. Experiments were performed on different device technologies using a large variety of sophisticated measurement and analysis techniques [5-8]. From the enormous amount of data different models have arisen capable of explaining characteristic NBTI features like the power law exponent, recovery, AC behavior, processing influence and many more [9-11]. The final aim of all these efforts is to develop know-how which helps to make better devices and better predictions for long term reliability under use conditions.

In this paper we focus on gated diode leakage currents due to trap assisted recombination at deep level defects at the Si/SiO_2 interface. The method is known as the direct-current current-voltage (DCIV) technique [12-13]. In planar MOSFETs DCIV is performed by measuring the substrate current when applying a forward bias (V_F) to the source/drain to substrate (bulk) junction. At certain gate biases deep level recombination becomes efficient at the Si/SiO_2 interface. Following [12], the maximum amplitude of the recombination current (ΔI_B) can be approximated as

$$\Delta I_B = \frac{\pi}{2}\frac{qA_G n_i \sigma_0 v_{th}}{2}\Delta N_{it}\exp\left(\frac{qV_F}{2kT}\right) \qquad (1)$$

In (1) q is the electronic charge, A_G is the effective gate area, n_i is the intrinsic carrier concentration, σ_0 is the average capture cross section $(\sigma_n\sigma_p)^{1/2}$ for electrons/holes, v_{th} is the medium thermal drift velocity and ΔN_{it} is the number of active recombination centers within a variable energy window $\Delta E_{it} = E_{Fn} - E_{Fp} \approx qV_F$. Assuming a homogeneous channel doping (i.e. no lightly doped drain (LDD) regions) and a flat density of states profile, we expect a single peak in the DCIV curve for a gate voltage that places the quasi Fermi levels for electrons (E_{Fn}) and holes (E_{Fp}) symmetric with respect to mid gap (E_i) → free electron density (n_S) = free hole density (p_S).

We perform electrical DCIV measurements at room temperature on 30nm and 5nm SiO_2 PMOS transistors after subjecting devices to negative bias temperature stress (NBTS). The stress temperature is provided by in-situ polyheaters embedding our test chip [14]. The transition from stress temperature to room temperature (RT) is performed by turning off the polyheater and waiting for the device to cool down. During cooing, the stress bias remains applied thereby freezing the degradation level (degradation quenching) [15]. We also perform spin dependent recombination (SDR) measurements at different gate biases in order to investigate the nature of the deep level defects contributing to the DCIV leakage current [16].

II. Electrical DCIV Results

A. *Basic Effect*

Fig.1 shows DCIV currents recorded (i) before stress, (ii) after subjecting the device to NBTS and (iii) after biasing the device for 100s in accumulation. The experiment was performed in a similar way on two devices with similar geometries but different gate oxide thicknesses. The 30nm SiO_2 device was stressed for 10s at a field of 6.0MV/cm and 400°C. The 5nm SiO_2 device was stressed for 1000s at a field of 7.4MV/cm and 280°C. The high stress temperatures (provided by polyheaters) allowed us to generate large defect densities within short stress times. We remark that the basic effects discussed in the following electrical measurements were verified for lower stress temperatures and longer stress times as well and turned out to be the same. This is consistent with recent research of some of us [17] demonstrating that the physics behind NBTI are essentially the same in 2.2nm SiON and 30nm SiO_2 devices within a temperature range of 0°C and 500°C. After NBTS, the DCIV current amplitude is considerably enhanced and we observe a negative threshold voltage shift in both devices consistent with the generation of positively charged defects, i.e. interface states and oxide traps. Charge pumping (CP) measurements (not shown) performed at the end of the experiment revealed trap densities of $D_{it}(30nm) \approx 7.6\times10^{11} eV^{-1}cm^{-2}$ and $D_{it}(5nm) \approx 6.7\times10^{11} eV^{-1}cm^{-2}$.

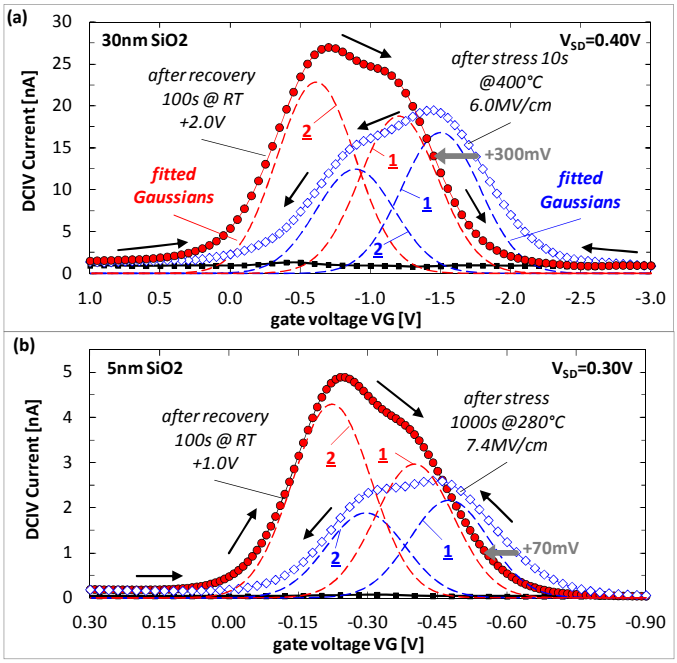

Figure 1. DCIV currents as a function of the gate voltage measured before NBTS (full squares), after NBTS when sweeping the gate bias from the negative stress voltage toward accumulation (open diamonds) and after 100s recovery in accumulation when sweeping the gate bias from accumulation back to inversion (full circles). Arrows indicate the directions of the gate voltage sweeps. All DCIV currents were recorded at RT. The elevated stress temperatures were provided by in-situ polyheaters. (a) shows data from a 30nm SiO_2 device stressed for 10s at 400°C and 6.0MV/cm. (b) shows data from a 5nm SiO_2 device stressed for 1000s at 280°C and 7.4MV/cm. Simulated Gaussians used to reproduce the DCIV spectrum are illustrated by dashed lines.

We observe the following features in both DCIV experiments: (i) when sweeping the gate voltage from inversion (coming from the negative stress voltage) toward accumulation, the DCIV traces show first a peak and then a shoulder. After remaining for 100s in accumulation and sweeping back to inversion, the DCIV traces have transformed showing a peak at the more positive and a shoulder at the more negative gate voltage. (ii) The DCIV amplitudes increased by 41% (30nm SiO_2) and 94% (5nm SiO_2) due to the positive gate voltage indicating the *generation of additional recombination centers at RT*. (iii) The threshold voltage shift decreased by about +300mV (30nm SiO_2) and +100mV (5nm SiO_2) due to the positive gate voltage indicating the *recovery of positively charged defects* consistent with the bulk of NBTI literature (i.e. [10]). The apparent conflict between (ii) and (iii) is resolved by assuming that the recovery of positively charged 'non-recombination defects' overshadows the creation of positively charged 'recombination defects'. We further remark: (I) Additional up/down sweeps (not shown) do not further change the shape of the DCIV curve. (II) From investigating the threshold voltage shift alone, the effect is not always obvious because the recovery of positive oxide charge typically overshadows the generation of D_{it}. (III) In a time resolved CP measurement performed after NBTS, the effect

can easily be overlooked too since CP requires averaging the current over a large number of accumulation-inversion sweeps (10,000 pulses using f=500kHz and t_{avg}=20ms). In an earlier study [18] we have shown that on a hydrogen-rich wafer the CP signal can actually increase within the first 100s after terminating stress. This is consistent with the DCIV data in Fig.1 which suggest the creation of recombination centers at positive gate bias after terminating stress.

To better understand the transformation of the DCIV traces, we attempted to reconstruct the double-peak feature before and after positive gate bias by two simulated Gaussians (labeled as peak 1 and peak 2) which have the same σ (σ(30nm)=280mV; σ(5nm)=85mV) but which are centered at different gate voltages and have different amplitudes. In the absence of LDD regions and under the assumption of a spatially homogeneous NBTI stress, two DCIV peaks at different gate biases are most likely due to two discrete defect levels with different σ_n/σ_p ratios and/or different energy positions in the silicon band gap. After applying the positive recovery bias for 100s their relative amplitudes change. In fact, it turns out that it is mostly peak 2 that increases due to the positive gate voltage.

B. Bias, time and temperature dependance

To study the phenomenon in more detail, we have performed additional electrical measurements on 30nm SiO_2 devices where we varied recovery bias, time and temperature *after NBTS*, cf. Fig.2. In (a), we switched for 1s to different gate voltages ranging from -0.5V to +4.0V. Afterwards, the gate bias was swept back to inversion while recording the DCIV current (just like in Fig.1). Peak 2 is found to increase with increasing recovery bias. In (b) we varied the time in accumulation (+2.0V) between 0.1s and 1000s and found that peak 2 increases with this time. In (c) we varied recovery and measurement temperature between 25°C and 200°C. Recovery was performed for 10s at +2.0V. Since elevating the temperature increases the diode forward current and the DCIV current amplitude, we used a smaller diode forward bias (+0.25V) and scaled the data to the maximum current. Peak 2 is found to increase with measurement/recovery temperature. The two peaks obviously behave very differently. While peak 1 is hardly affected by the particular recovery condition, peak 2 increases.

Post-stress creation of interface defects at RT was explained previously by hydrogen transport models where atomic (H^0) or ionic hydrogen (H^+) gets released from Si-H precursors during irradiation. When applying a positive gate bias after stress hydrogen may re-approach the interface and depassivate Si-H bonds [19-20]. It was shown by Rashkeev *et al.* [21] using first-principles density functional calculations that H^+ is the only stable charge state at the interface and that it may react readily with Si-H bonds forming H_2 molecules and positively charged dangling bonds (P_b centers). Stathis *et al.* [22] suggested that the two P_b center variants at the silicon (100) interface (P_{b1} & P_{b0}) react differently with hydrogen, the latter being more efficiently generated by hydrogen reactions. Due to the similarities between our observations and the standard model for irradiation damage, we suspect that hydrogen may play a crucial role in the reported DCIV dynamics.

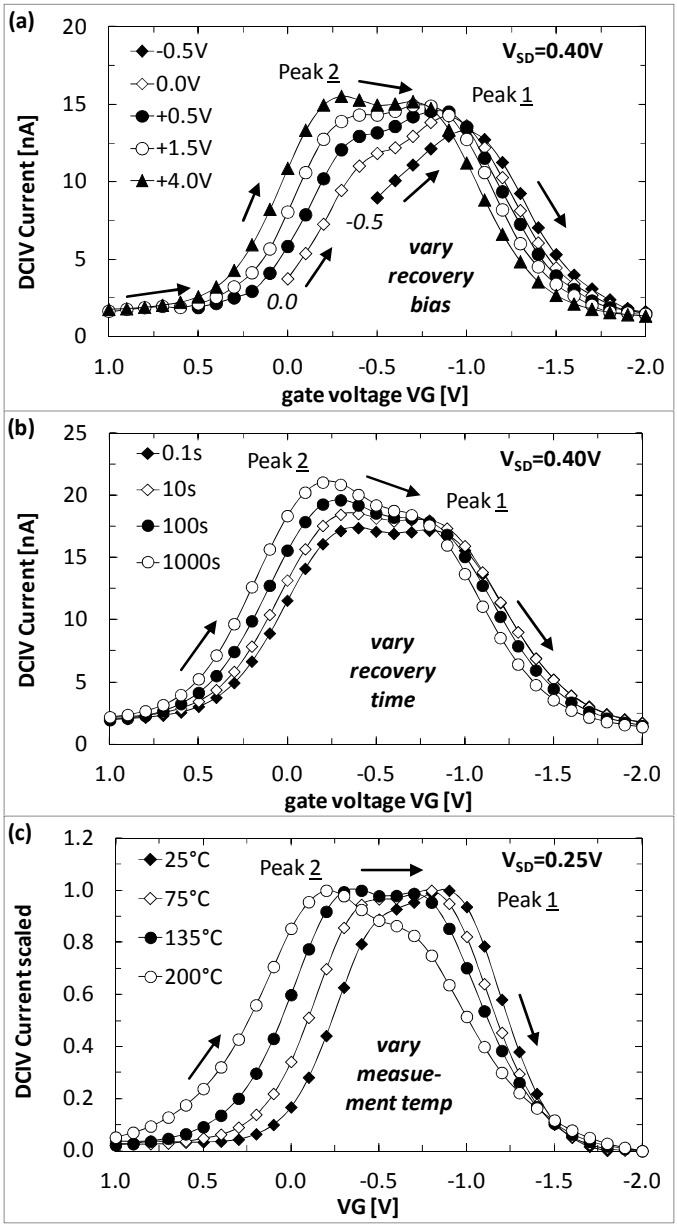

Figure 2. A study of the DCIV line shape (on 30nm SiO_2 devices) as a function of the recovery bias (a), the recovery time (b) and the recovery/measurement temperature (c). Data in (a) and (b) were recorded at RT after NBTS. Elevated measurement temperatures in (c) and the stress temperature in (a), (b) and (c) were applied in-situ using the polyheater technique. NBTS was performed for 10s at 6.0MV/cm and 400°C. Peak 1 is hardly affected by the particular recovery condition. Peak 2 becomes bigger the more positive the recovery bias, the longer the recovery time and the higher the recovery temperature.

III. COMBINED DCIV/SDR EXPERIMENT

The only measurement method with the analytical power to enhance our understanding at this point is electrically detected magnetic resonance (EDMR) by SDR. Earlier studies have already demonstrated the analytical power of SDR in silicon and silicon carbide based MOSFETs [23-24]. In pioneering work of Campbell *et al.* [24-25] NBTS, DCIV current measurements and SDR were performed serially and independent of each other with undefined recovery and device-floating periods in-between. In this study we combine everything in one single experiment.

A. Experimental Setup for the DCIV/SDR experiment

The transition from the electrical measurement to SDR is performed on-the-fly with all junction biases remaining applied. This was accomplished by placing the device in a tuned microwave cavity for the entire experiment. We glued the test chip on a PCB sample holder (a so called 'T') and wire-bonded the transistor pads to gold leads deposited on this 'T'. The gold leads were soldered to BNC cables which were connected to the source-measure units (SMUs) of a conventional semiconductor parameter analyzer (SPA). The transition from the electrical DCIV measurement to SDR was performed by unplugging the substrate BNC from the 0.0V SMU of the SPA and feeding the current into a current pre-amp. Using magnetic field modulation of 2G at 1kHz and a lock-in system, we filtered the spin depended components form the DCIV current and recorded the SDR amplitude as a function of the magnetic field. SDR was performed at X-band using a microwave frequency of about 9.2GHz.

B. DCIV/SDR results

The DCIV current in our combined DCIV/SDR experiment is illustrated in Fig.3 (a). The difference with respect to Fig.1 is (besides the lower stress temperature of 200°C and the longer stress time) that the DCIV sweep has been interrupted several times at certain gate voltages in order to perform a SDR measurement. After the SDR experiment the substrate BNC was switched back to the SPA and the DCIV gate voltage sweep was continued. We interrupted the DCIV sweep four times to record SDR traces before stress (SDR0), after stress at the maximum of the DCIV curve (SDR1-), after 100s recovery (+2.0V) at peak 2 (SDR2+) and at peak 1 (SDR1+). The SDR breaks (each about 24h signal averaging) caused some recovery in the DCIV current, visible as steps in (a). However, the basic features of the DCIV current maintained conserved. After completion of the combined DCIV/SDR experiment, we recorded a final CP curve in (b) which revealed an interface state defect density of $D_{it}\approx 9.8\times10^{11}eV^{-1}cm^{-2}$ consistent with the large increase in the DCIV current amplitude.

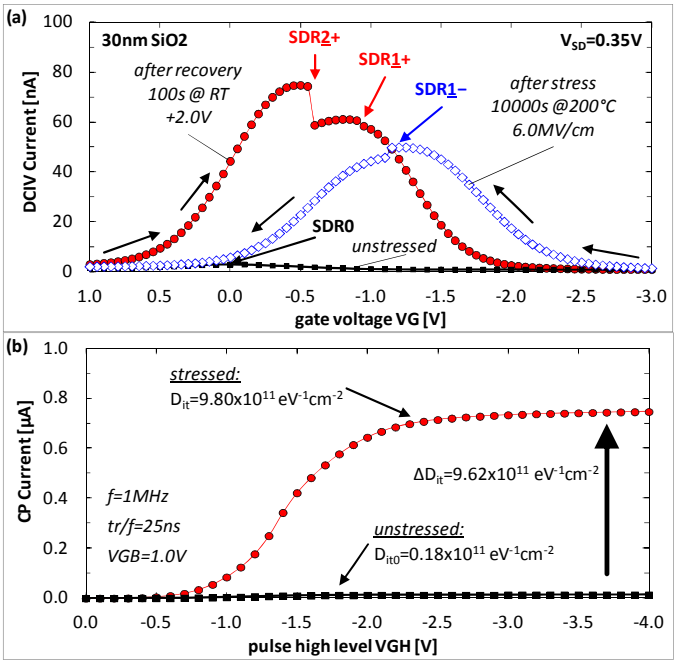

Figure 3. (a) illustrates DCIV currents as a function of the gate voltage similar as in Fig.1. NBTS was performed for 10,000s at 200°C (6.0MV/cm) using the polyheater technique. At certain gate biases the DCIV sweep was interrupted and a SDR measurement was performed. The gate biases at which SDR measurements were performed are indicated as SDR0 (unstressed), SDR1− (after NBTS at peak 1), SDR2+ (after +2.0V at peak 2) and SDR1+ (after +2.0V at peak 1). The device was in the resonance cavity during the entire measurement. In (b) we show a CP measurement before stress (full squares) and at the end of the combined DCIV/SDR experiment (full circles). Due to NBTS the D_{it} increased from 0.18×10^{11} $eV^{-1}cm^{-2}$ to 9.80×10^{11} $eV^{-1}cm^{-2}$.

The SDR results are illustrated in Fig.4. In SDR0 (before stress) the defect density was below our detection limit ($D_{it0}\approx1.8\times10^{10}eV^{-1}cm^{-2}$). In SDR1- we detect a signal which shows a center g value of about 2.0069. This is close to the g value reported for P_{b0} centers (2.0060) [26] (We have also rotated the device in the magnetic field (not shown) and verified that the shift in the g value qualitatively follows the one reported for the P_{b0} center). Symmetric to the center line we detect hyperfine (HF) side structure indicating a *second* similar defect where the defect's electron wave function overlaps with spin 1/2 paramagnetic nuclei, most likely hydrogen.

IV. DISCUSSION

It is unlikely that the observed HF doublet is due to previously reported E'center-hydrogen complexes like the 10.4G or the 74G doublets [27-30]. As shown in [27-30], such HF doublets would appear almost perfectly symmetric to the regular silicon E'center line (g value 2.0005) with effective g values of about 2.0005 (10.4G) and 2.0014 (74G). The reported HF doublet appears, however, symmetric to the P_{b0} line (g value 2.0069). Thus, a more plausible defect explaining the observed HF side peaks would be a P_b center-hydrogen complex.

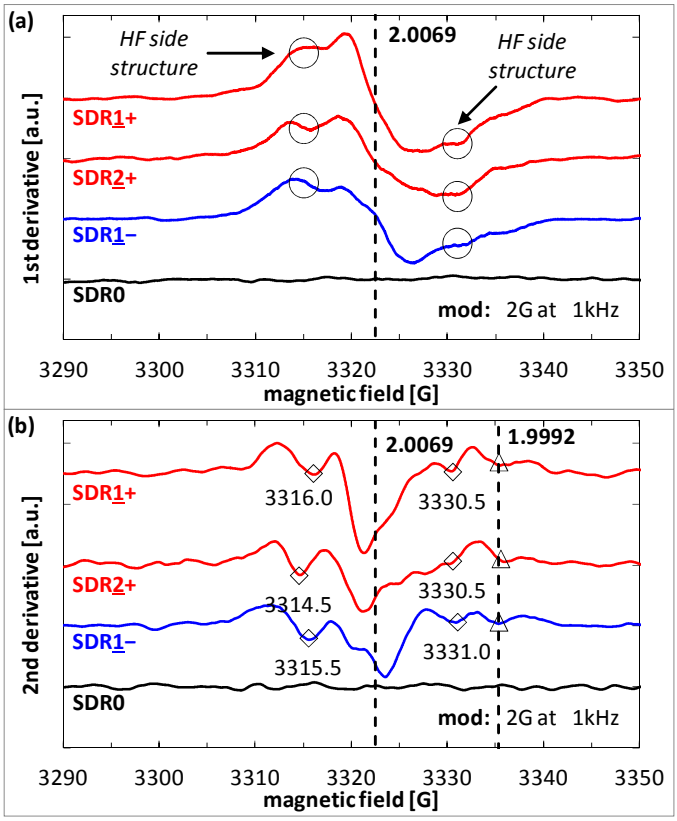

Figure 4. (a) Four SDR traces corresponding to the four different operating points shown in Fig.3. The center line has a g value of 2.0069 suggesting regular P_{b0} centers as the main defect. Symmetric HF side peaks (separated by 15G) indicate a second similar defect coupled to hydrogen (i.e. a P_b center-hydrogen complex). Due to recovery at +2.0V the intensity of the center line becomes larger. (b) illustrates the second derivative of the SDR signal. Different lines show up more obvious as minima. SDR was performed in X band (9.2GHz).

Using density functional theory calculations Tuttle *et al.* [31] and Alkauskas *et al.* [32] found that the Si-H bond at the Si/SiO_2 interface has a meta-stable (~0.5eV deep) state in the antibonding and/or in the bridging configuration giving rise to an additional energy level in the *upper* half of the silicon band gap. In the meta-stable state hydrogen is released easily by (i) recombining with H^+ (thereby forming H_2) or (ii) by charging the adjacent dangling bond. In [33] some of us recently found such an energy level in the upper half of the band gap which showed almost exactly the same features as peak 2 in the DCIV experiment. If a hydrogen atom is close enough to the dangling bond of the P_b center, the original spectrum splits up symmetric to the center line because the magnetic moment of the nucleus can either line up or oppose the applied quasi-static magnetic field. Similar HF structure as in SDR1- appears also in SDR2+ and SDR1+. The integrated intensities of SDR2+ and SDR1+ are, however, bigger than the one of SDR1- which is consistent with the larger DCIV current measured after positive gate voltage. Also, the center lines of SDR2+ and SDR1+ are stronger in comparison to their HF side peaks suggesting less P_b center hydrogen-complexes and larger number of 'regular' P_b centers. This is consistent with the assumption of enhanced release of hydrogen from P_b center-hydrogen complexes at positive gate bias. Upon H-release P_b center-hydrogen complexes would simply transform into regular P_b centers (center line). The excellent signal/noise ratio allowed us to investigate the second derivative of the SDR spectrum as well where individual signals appear more obvious as minima, cf. Fig.4 (b). The dominating HF interaction (which is most likely due to hydrogen) was found to be about 15G. We also find a hint for a signal around 3335G. The g value of this signal is 1.9992 which is close to the g values reported for E' centers (2.0005).

V. Conclusions

We have presented DCIV and SDR data that indicate two different P_b center-like defects after NBTS. In electrical DCIV measurements performed after NBTS we have studied the bias, time and temperature dynamics of defect creation and recovery and found that the two variants behave very differently. While defect 1 is hardly affected by the particular recovery condition, defect 2 increases with accumulation bias, recovery time and temperature. SDR measurements identify the first defect as a regular P_{b0} center while the second defect is most likely a P_b center-hydrogen complex.

Acknowledgment

The work at Penn State was also supported in part by Infineon Technologies Austria. The work at Penn State was also supported by the U.S. Department of Commerce under Award No. NIST 60NANB10D109 and the US Army Research Laboratory. Any opinions, findings, conclusions, or other recommendations expressed herein are those of the authors and do not necessarily reflect the views of the U.S. Commerce Department or the US Army Research Laboratory.

References

[1] K. O. Jeppson, and C. M. Svensson, "Negative bias stress of MOS devices at high electric fields and degradation of MOS devices," J. Appl. Phys. vol. **48**, 1977, pp. 2004-2014.

[2] T. Grasser, B. Kaczer, W. Goes, H. Reisinger, T. Aichinger, P. Hehenberger, P.-J. Wagner, F. Schanovsky, J. Franco, P. Roussel, and M. Nelhiebel, "Recent advances in understanding the bias temperature instability," IEEE *International Electron Devices Meeting* (IEDM) 2010, pp. 4.4.1-4.4.4.

[3] D. K. Schroder, "Negative bias temperature instability: What do we understand?" Microelectron. Reliab. vol. **94**, 2007, pp. 841-852.

[4] J. H. Stathis, and S. Zafar, "The negative bias temperature instability in MOS devices: A Review," Microelectron. Reliab. vol. **46**, 2006, pp. 270-286.

[5] A. E. Islam, E. N. Kumar, H. Das, S. Purawat, V. Maheta, H. Aono, E. Murakami, S. Mahapatra, and M. A. Alam, "Theory and practice of on-the-fly and ultra-fast VT measurements for NBTI degradation: challenges and opportunities," IEEE *International Electron Devices Meeting* (IEDM) 2007, pp. 805-808.

[6] H. Reisinger, O. Blank, W. Heinrigs, W. Gustin, and C. Schlünder, "A comparison of very fast to very slow components in degradation and recovery due to NBTI and bulk hole trapping to existing physical models," IEEE *Trans. Device Mater. Reliab.* vol. 7, 2007, pp. 119-129.

[7] M.-F. Li, D. Huang, C. S. Yang, T. Liu, and W. J. Zhiying Liu, "Understand NBTI Mechanism by Developing Novel Measurement Techniques," IEEE Trans. Device Mater. Reliab. vol. **8**, 2008, pp. 62-71.

[8] T. Grasser, H. Reisinger, P. Wagner, F. Schanovsky, W. Goes, and B. Kaczer, "The time dependent defect spectroscopy (TDDS) for the characterization of the bias temperature instability," IEEE *International Reliability Physics Symposium* (IRPS) 2010, pp. 16-25.

[9] M. A. Alam, and S. Mahapatra, "A comprehensive model of PMOS NBTI degradation," Microelectron. Reliab. vol. **45**, 2005, pp. 71-81.

[10] V. Huard, M. Denais, F. Perrier, N. Revil, C. Parthasarathy, A. Bravaix, and E. Vincent, "A thorough investigation of MOSFETs NBTI degradation," Microelectron. Reliab. vol. **45**, 2005, pp. 83-98.

[11] T. Grasser, B. Kaczer, W. Goes, T. Aichinger, P. Hehenberger, and M. Nelhiebel, "A two-stage model for negative bias temperature instability," IEEE *International Reliability Physics Symposium* (IRPS) 2009, pp. 33-44.

[12] A. Neugroschel, C.-T. Sah, K. M. Han, M. S. Carroll, T. Nishida, J. T. Kavalieros, and Y. Lu, "Direct-current measurements of oxide and interface traps on oxidized silicon," IEEE Trans. Electron Devices vol. **42**, 1995, pp.1657-1662.

[13] C.-T. Sah, A. Neugroschel, K. M. Han, and J. T. Kavalieros, "Profiling interface traps in MOS transistors by the DC current-voltage method," IEEE Electron Device Lett. vol. **17**, 1996, pp. 72-74.

[14] T. Aichinger, M. Nelhiebel, S. Einspieler, and T. Grasser, "In situ poly heater—A reliable tool for performing fast and defined temperature switches on chip," IEEE Trans. Device Mater. Reliab. vol. **10**, 2009, pp.3-8.

[15] T. Aichinger, M. Nelhiebel, and T. Grasser, "On the temperature dependence of NBTI recovery," Microelectron. Reliab. vol. **48**, 2008, pp. 1178-1184.

[16] P. M. Lenahan, and M. A. Jupina, "Spin dependent recombination at the silicon/silicon dioxide interface," Colloids Surf. vol. **45**, 1990, pp. 191-211.

[17] G. Pobegen, T. Aichinger, M. Nelhiebel, and T. Grasser, "Understanding Temperature Acceleration for NBTI," IEEE *International Electron Devices Meeting* (IEDM) 2012

[18] T. Grasser, T. Aichinger, G. Pobegen, H. Reisinger, P.-J. Wagner, F. Franco, M. Nelhiebel, and B. Kaczer, "The 'permanent' component of NBTI: Composition and annealing," IEEE *International Reliability Physics Symposium* (IRPS) 2011, pp. 6A.2.1-6A.2.9.

[19] F. B. McLean, "A Framework for Understanding Radiation-Induced Interface States in SiO2 MOS Structures," IEEE Trans. Nucl. Sci. vol. **27**, 1980, pp. 1651-1657.

[20] D. B. Brown, and N. S. Saks, "Time dependence of radiation‐induced interface trap formation in metal‐oxide‐semiconductor devices as a function of oxide thickness and applied field," J. Appl. Phys. vol. **70**, 1991, pp. 3734-3747.

[21] S. N. Rashkeev, D. M. Fleetwood, R. D. Schrimpf, and S. T. Pantelides, "Defect Generation by Hydrogen at the Si- SiO_2 Interface," Phys. Rev. Lett. vol. **87**, 2001, pp. 165506-1-165506-4.

[22] J. H. Stathis, and E. Cartier, "Atomic hydrogen reactions with P_b centers at the (100) Si/SiO_2 interface," Phys. Rev. Lett. vol. **72**, 1994, pp. 2745-2748.

[23] C. J. Cochrane, P. M. Lenahan, and A. J. Lelis, "An electrically detected magnetic resonance study of performance limiting defects in SiC metal oxide semiconductor field effect transistors," J. Appl. Phys. vol. **109**, 2011, pp. 014506-1-014506-12.

[24] J. P. Campbell, P. M. Lenahan, A. T. Krishnan, and S. Krishnan, "Observations of NBTI-induced atomic-scale defects," IEEE Trans. Device Mater. Reliab. vol. **6**, 2006, pp. 117-122.

[25] J. P. Campbell, P. M. Lenahan, C. J. Cochrane, A. T. Krishnan, and S. Krishnan, "Atomic-Scale defects involved in the negative-bias temperature instability," IEEE Trans. Device Mater. Reliab. vol. **7**, 2007, pp. 540-557.

[26] Y. Y. Kim, and P. M. Lenahan, "Electron‐spin‐resonance study of radiation‐induced paramagnetic defects in oxides grown on (100) silicon substrates," J. Appl. Phys. vol. **64**, 1988, pp. 3551-3557.

[27] J. F. Conley, and P. M. Lenahan, "Molecular hydrogen, E' center hole traps, and radiation induced interface traps in MOS devices," IEEE Trans. Nucl. Sci. vol. **40**, 1993, pp. 1335-1340.

[28] J. F. Conley, and P. M. Lenahan, "Electron Spin Resonance Analysis of EP Center Interactions With H_2: Evidence for a Localized EP Center Structure," IEEE Trans. Nucl. Sci. vol. **42**, 1995, pp. 1740-1743.

[29] J. Vitko, "ESR Studies of Hydrogen Hyperfine Spectra in Irradiated Vitreous Silica," J. Appl. Phys. vol. **49**, 1978, pp. 5530-5535.

[30] T. E. Tsai, and D. L. Griscom, "On the Structures of Hydrogen Associated Defect Centers in Irradiated High-Purity a-SiO_2:OH," J. Non-Cryst. Solids vol. **91**, 1987, pp. 170-179.

[31] B. Tuttle, and C. G. Van de Walle, "Structure, energetics, and vibrational properties of Si-H bond dissociation in silicon," Phys. Rev. B: Condens. Matter vol. **59**, 1999, pp. 12884-12889.

[32] A. Alkauskasa, and A. Pasquarello, "Alignment of hydrogen-related defect levels at the Si-SiO_2 interface," Phys. B vol. **401–402**, 2007, pp. 546-549.

[33] T. Aichinger, M. Nelhiebel, S. Decker, and T. Grasser, "Energetic distribution of oxide traps created under negative bias temperature stress and their relation to hydrogen," Appl. Phys. Lett. vol. **96**, 2010, pp. 133511-1-133511-3.